8 High Lift Systems and Maximum Lift Coefficients

In Section 7 the wing was examined with flaps retracted (clean wing). According to the assumptions from Section 5, the wing is, however, supposed to achieve higher lift coefficients on take-off and landing. This is facilitated by high lift systems on the wing. Subsection 8.1 will show what types of high lift system are used and the characteristics of the different versions.

Subsection 8.2 deals with the approximate calculation of the maximum lift coefficients from the geometrical parameters, which are assumed to be known, of the high lift systems.

Subsection 8.3 shows how this analytical method of calculation can be inverted for the design of the high lift system. It is demonstrated how the characteristic geometrical parameters for describing the high lift system can be calculated from the lift coefficients for take-off and landing selected in Section 5.

8.1 High Lift Systems

High lift systems operate according to the following principles:

- Increasing the airfoil camber.
- Boundary layer control by:
    - improving pressure distribution;
    - feeding high-energy airflow to the boundary layer;
    - removing the "old" boundary layer.
- Increasing the wing area.

A distinction is made between:

- active high lift systems;
- passive high lift systems.

This description is restricted to the typical passive high lift systems, which do not require any additional equipment apart from the drive system for retracting and extending the flaps.

In the history of aircraft development every conceivable alternative has been put to the test to increase lift. Fig. 5.4, Fig. 8.1 and Fig. 8.3 only describe the versions that have established themselves in practice.

Trailing edge high lift systems

The **plain flap** (Fig. 8.1) is simply a pivoted rear section of an airfoil. Typically the flap depth c_F amounts to 30% of the chord. The plain flap increases lift by increasing the airfoil camber. Ailerons, elevators and rudders are plain flaps.

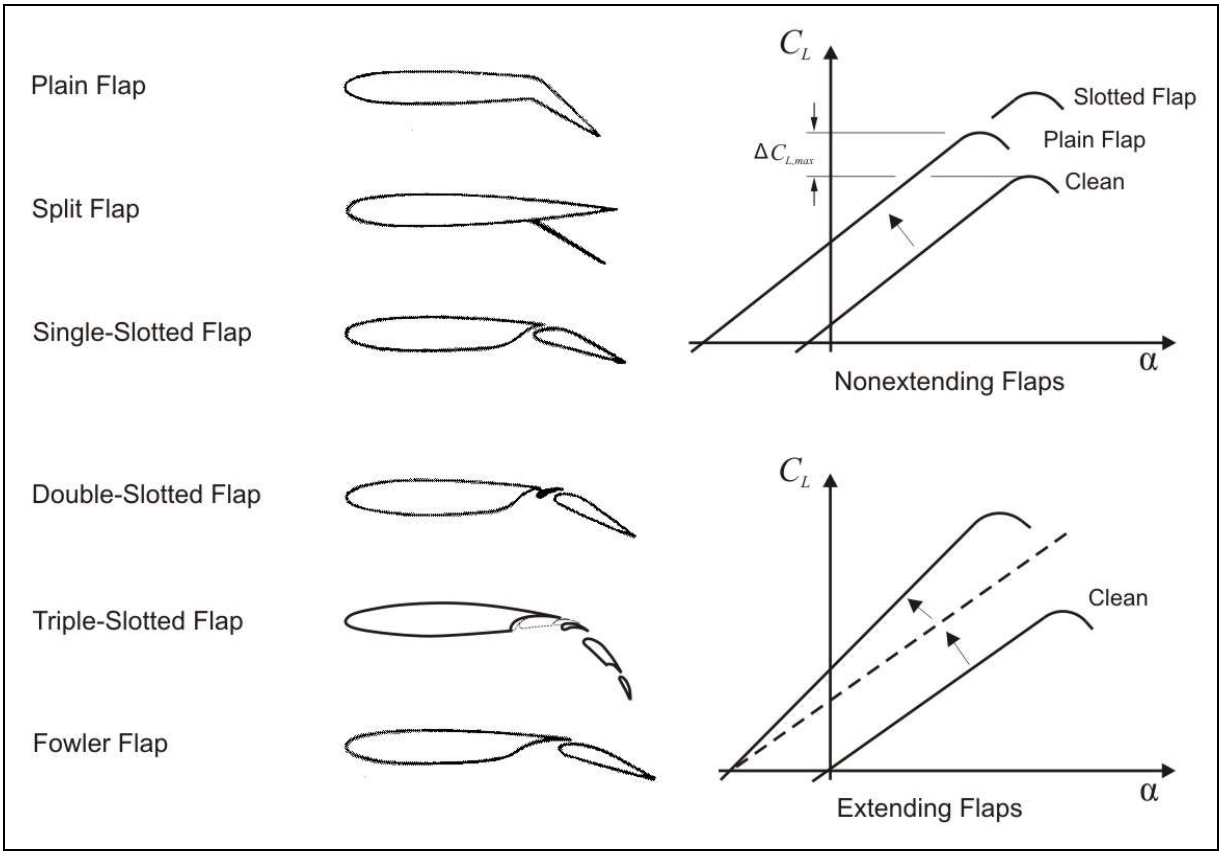

Fig. 8.1 Different trailing edge high lift systems (airfoils from **DATCOM 1978**)

Split flaps are no longer used because they produce more drag than a plain flap with the same increase in lift.

The **slotted flap** gets its name from the slot between the wing and the flap. Air can flow from the bottom to the top of the airfoil through the specially shaped slot. This high-energy flow produces a new boundary layer on the top surface of the flap, which allows flap angles of up to 40° without separating the flow. Consequently maximum lift is increased and drag is reduced by the slot.

Fowler flaps have a slot between the wing and flap like slotted flaps.

- *Fowler flaps are first extended to the rear,* thus increasing the wing area. With increasing wing area the lift becomes greater. If the reference area S_{ref} is now kept constant in the lift equation $L = 1/2 \rho v^2 \cdot C_L \cdot S_{ref}$, the lift coefficient increases (by definition). By moving the Fowler flap downwards, the lift is increased without a disproportionate increase in drag. The corresponding flap position is therefore especially suited to take-off.

- If the Fowler flap is further extended, the *flap body is also turned downwards*, which now increases the airfoil camber. The lift continues to increase, but now with a greater increase in drag. The corresponding flap position is therefore suitable for landing.

Three types of **flap kinematics** are used (Fig. 8.2):

- Flaps can be deflected via a **dropped hinge** system. The flap's pivot is under the wing.
- If an aerodynamically optimum slot geometry is required for all flap positions, this cannot be achieved with a dropped hinge system, as a rule. A different (more complex) version offers more possibilities: the flap is mounted on a carriage, which is moved on a **track**.
- A third type of flap design, essentially as a compromise between the two versions above, works with a **linkage** system.

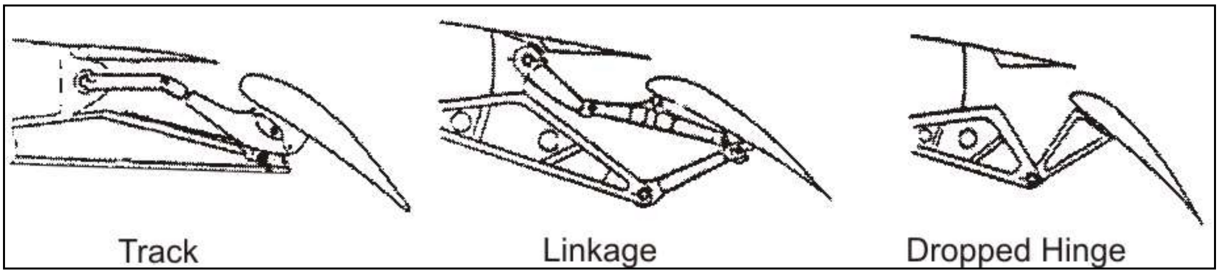

Fig. 8.2 Flap kinematics of high lift systems

In the case of all high lift mechanisms it must be borne in mind that the flap mountings have to be housed in fairings. The fairings represent an additional drag throughout the entire flight, which can compromise the advantages of the high lift system.

To further improve the flow over the flap, **double slotted flaps** or even **triple slotted flaps** can be used.

Leading edge high lift systems

If a fixed slat is placed in front of the wing's leading edge, a **leading edge slot** (Fig. 8.3) is produced between the leading edge and the wing. As is the case for the slot of a landing flap, a high-energy flow is exerted on the top surface of the airfoil, although this is not to facilitate a bigger camber, but rather to utilize a higher angle of attack for the existing camber of the wing profile.

A **leading edge flap** increases the curvature of the top of the airfoil. This considerably increases the lift coefficient.

A movable **slat (slotted leading edge flap)** increases the lift through a combination of increased wing area and increased camber and through the influence of the flow with the aid of the slat.

A **Kruger flap** forces the flow to run more over the top of the airfoil. Kruger flaps can be built more easily and made more lightweight than slats, but the disadvantage is their high level of drag at small angles of attack. In the case of large passenger aircraft Kruger flaps are often used on the inner wing together with slats on the outer wing.

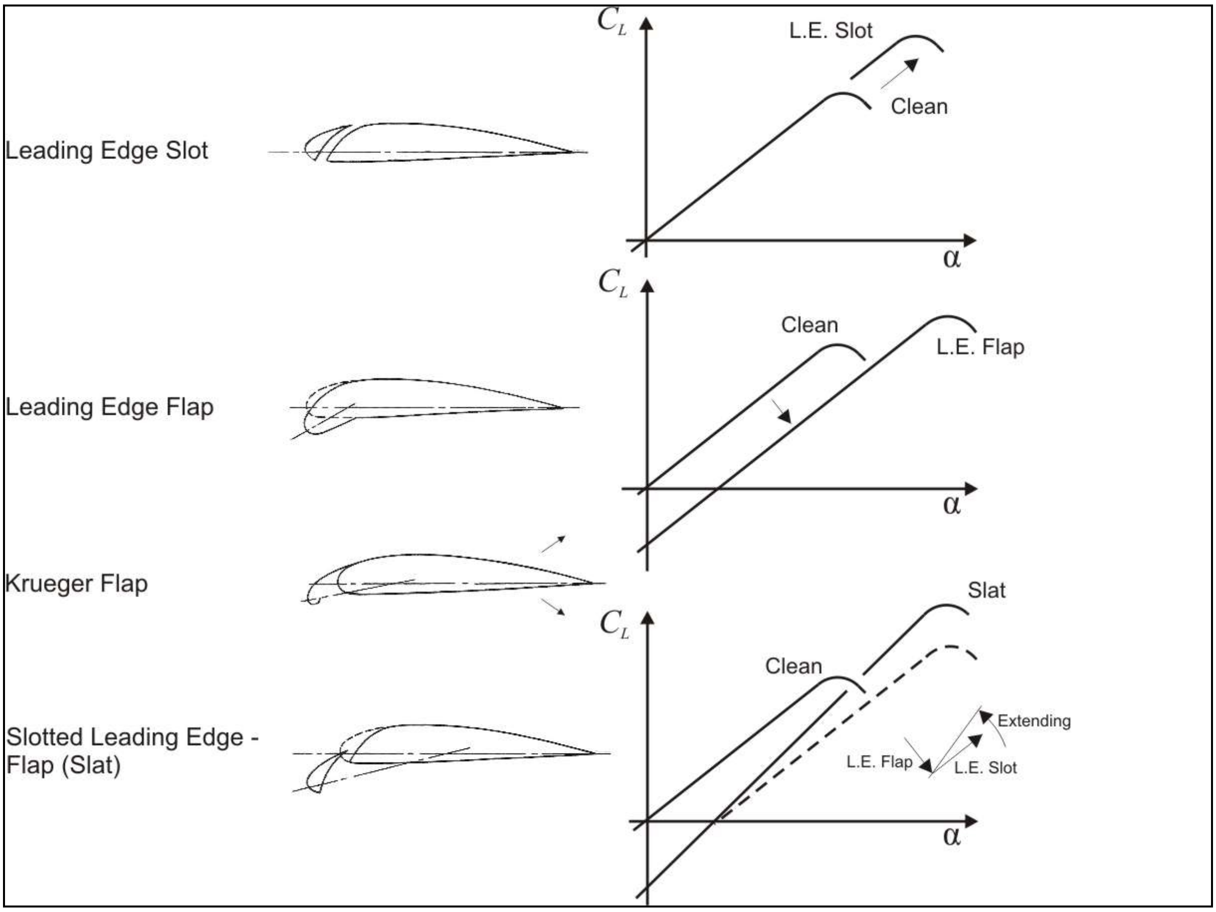

Fig. 8.3 Different leading edge high lift systems (airfoils from **DATCOM 1978**)

Generation of high lift

A comparison of the mode of operation of high lift systems is shown in Fig. 8.1 and Fig. 8.3. The lift curve of plain and slotted flaps is elevated to higher lift coefficients compared to the lift curve without flaps, but without increasing the stall angle. On the contrary, the stall angle tends to be smaller. In order to increase the lift through higher angles of attack (without airflow separation), high lift systems are inserted on the leading edge. A higher lift curve slope is ascertained for flaps and slats, which increase the wing area.

To sum up, it can be stated that effective high lift systems have a more complicated design than simple and less effective systems, and this leads to higher acquisition and maintenance costs. On the other hand, the more effective system saves fuel through the possibility of building a lighter wing with better lift-to-drag ratio than would be possible in the case of an overall design with a simple high lift system. An optimum compromise can – as is so often the case – only be found through detailed studies. In the early stages of design it is therefore advisable to follow the designs of successful aircraft models.

8.2 Calculation of Maximum Lift Coefficients

Fig. 8.4 shows a typical lift curve $c_L = f(\alpha)$. α is the angle of attack, which is defined as the angle between the free – i.e. undisturbed – flow direction and the chord line of the airfoil without a flap deflection. With an angle of attack of 0° the uncambered airfoil does not show any lift. The cambered airfoil, on the other hand, already has a certain lift coefficient with an angle of attack of $\alpha = 0$, and also achieves a higher maximum lift coefficient. The zero-lift angle of attack α_0 is negative in the case of an airfoil with a positive camber. The lift curve slope $c_{L\alpha}$ is constant apart from a small section just before the stall angle $\alpha_{c_{L,max}}$.

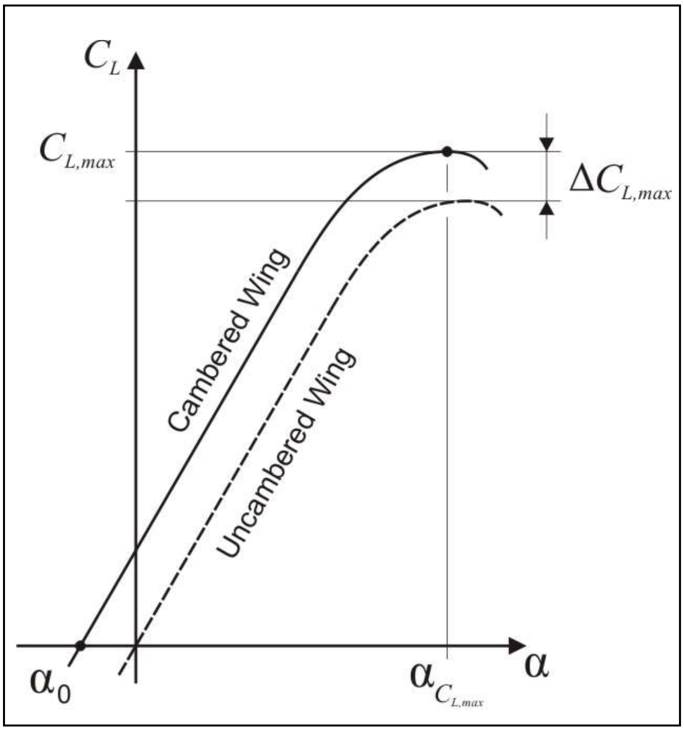

Fig. 8.4 Lift curve comparing an cambered and an uncambered wing

The maximum lift coefficient of an airfoil

For the following calculations the maximum lift coefficient of an airfoil from wind tunnel tests should be known. **Airfoil catalogs** such as **Abbott 1959** contain measured lift, drag and pitching moment coefficients of airfoils for various angles of attack and may serve as a starting point for further calculations.

If, exceptionally, no wind tunnel data or airfoil catalogs are available, it is possible to estimate the maximum lift coefficient according to **DATCOM 1978 (4.1.1.4)**:

$$c_{L,max,clean} = \left(c_{L,max}\right)_{base} + \Delta_1 c_{L,max} + \Delta_2 c_{L,max} + \Delta_3 c_{L,max} \quad . \tag{8.1}$$

$\Delta_1 c_{L,max}$ Correction term for taking into account the airfoil camber and the position of maximum camber. Position of maximum thickness: 30%.

$\Delta_2 c_{L,max}$ Correction term for taking into account a position of maximum thickness $\neq$ 30%

$\Delta_3 c_{L,max}$ Correction term for taking into account the influence of Reynolds' number $\neq 9 \cdot 10^6$.

Additional corrections would be necessary to take into account the roughness of the airfoil surface and the Mach number. However, these corrections cannot be stated with universal validity.

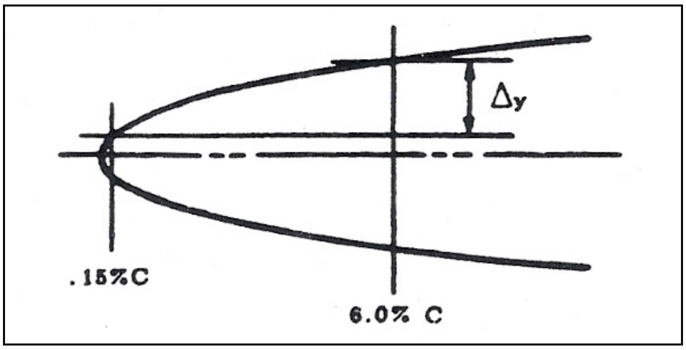

Fig. 8.5 Definition of the leading-edge sharpness parameter Δy (**DATCOM 1978**)

The maximum lift coefficient of a wing depends on the *leading-edge sharpness parameter* Δy, which is defined in Fig. 8.5:

- in the case of a sharp airfoil leading edge (i.e. small Δy) the flow starts to separate at the airfoil leading edge.
- in the case of a more rounded airfoil leading edge (i.e. large Δy) the flow starts to separate at the airfoil trailing edge.

In the case of known NACA airfoils, Δy can be directly determined from the maximum relative thickness with the aid of Table 8.1.

Table 8.1: Δy -parameter for known NACA airfoils determined from **DATCOM 1978** (2.2.1-8)

Airfoil type	Δy
NACA 4 digit	$26.0 \cdot (t/c)$
NACA 5 digit	$26.0 \cdot (t/c)$
NACA 63 series	$22.0 \cdot (t/c)$
NACA 64 series	$21.3 \cdot (t/c)$
NACA 65 series	$19.3 \cdot (t/c)$
NACA 66 series	$18.3 \cdot (t/c)$

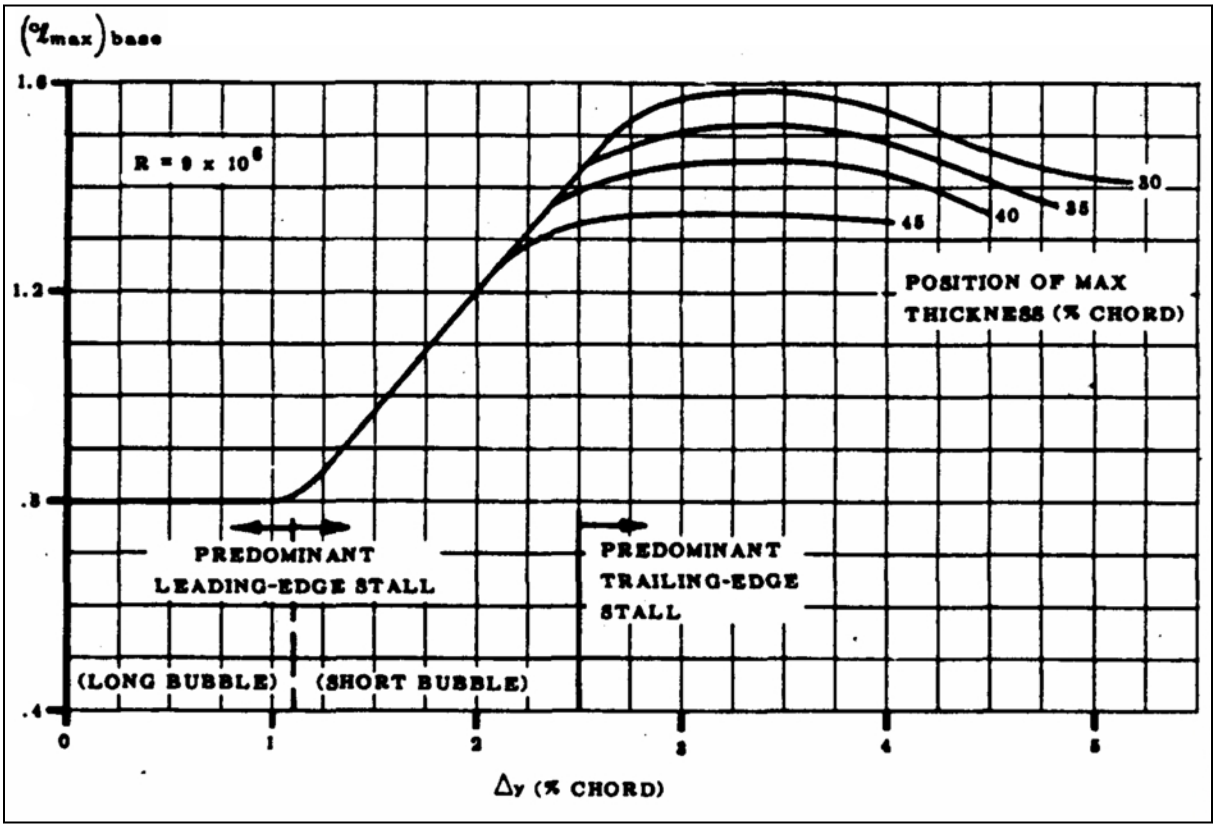

Fig. 8.6 Maximum lift coefficient of a symmetrical airfoil at a Reynolds' number of $9 \cdot 10^6$ as a function of Δy and the position of maximum thickness

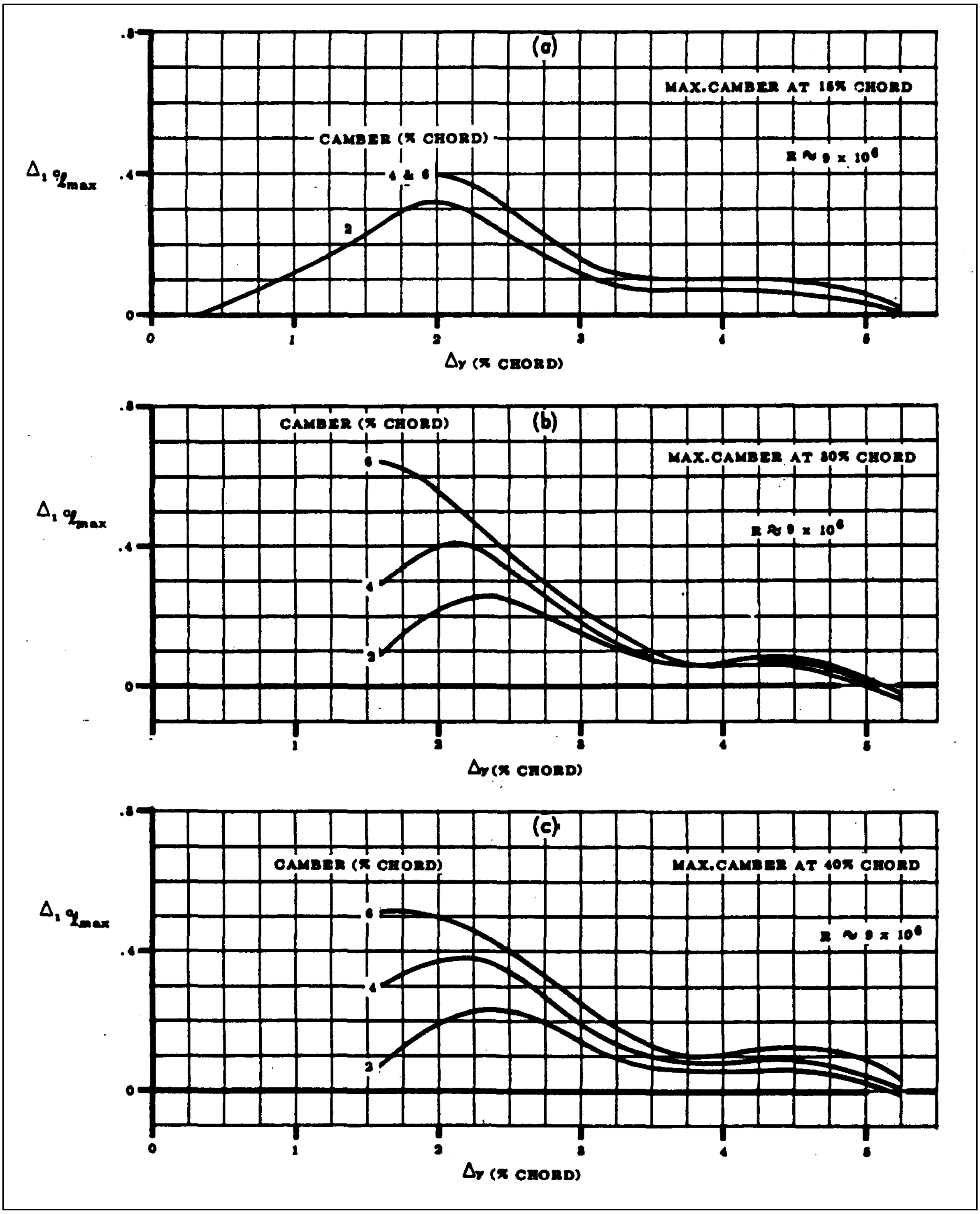

Fig. 8.7 Correction term $\Delta_1 c_{L,max}$ to calculate the maximum lift coefficient of an airfoil according to **DATCOM 1978**. Considered are airfoil camber and position of maximum camber.

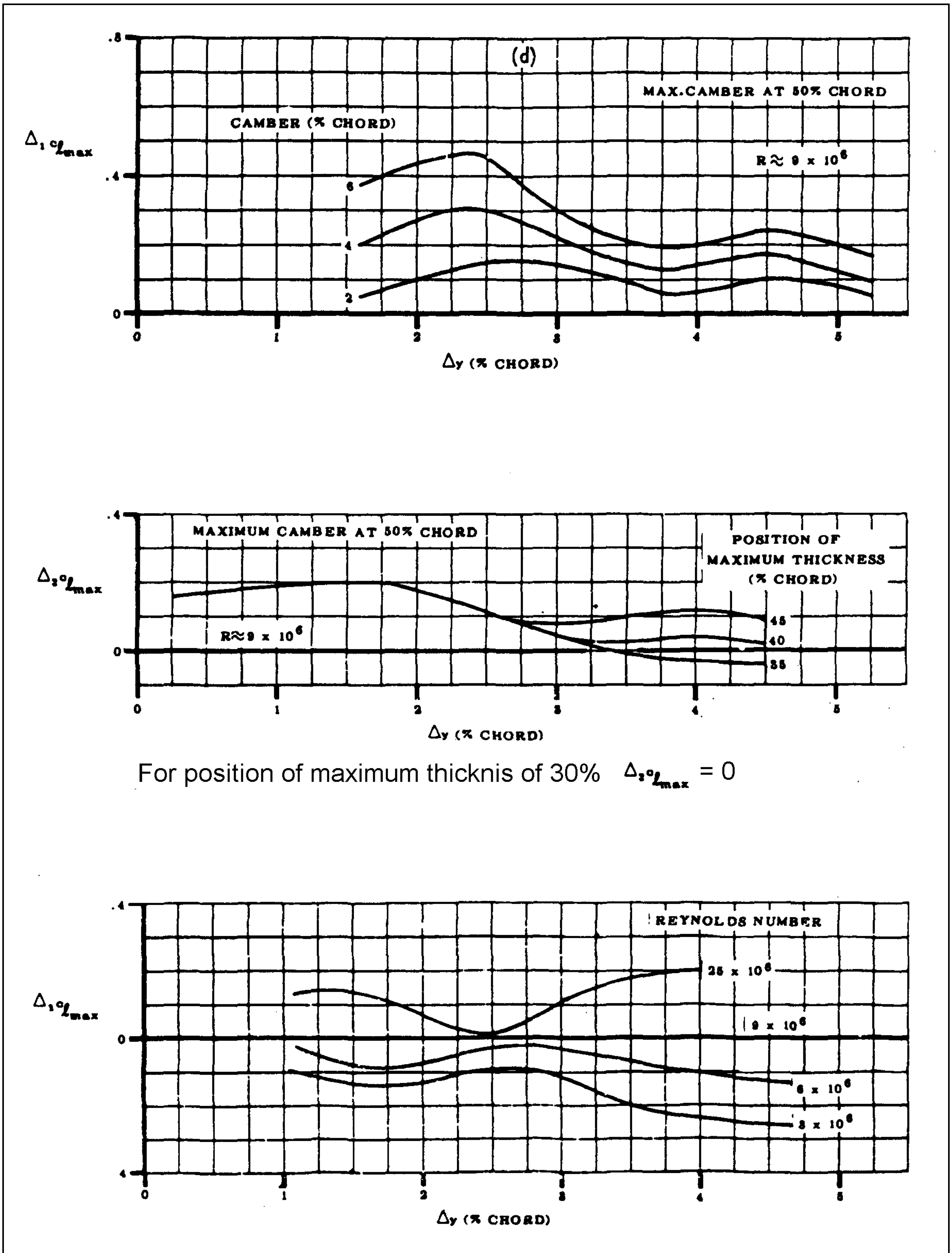

Fig. 8.8 Correction terms to calculate the maximum lift coefficient of an airfoil according to **DATCOM 1978**.

Above: Figure 8.7 continued

Middle: $\Delta_2 c_{L,max}$: Correction term for the position of maximum thickness

Below: $\Delta_3 c_{L,max}$: Correction term for the influence of Reynolds' number

The maximum lift coefficient of a wing

With high angles of attack and a sharp airfoil leading edge (i.e. small Δy), the flow starts to separate at the airfoil leading edge. The resulting vortexes can lead to an *increase* in the maximum lift coefficient of a swept wing compared to an unswept wing. A dorsal fin, as a transition to the vertical tailplane (compare, for example, Fig. 4.6), achieves an increase in maximum lift coefficient by means of the process described. In doing so, the large sweep angle of the dorsal fin is of importance.

On the other hand, many of the airfoils used in commercial aircraft have a more rounded airfoil leading edge (i.e. a large Δy). This is the case, for example, on supercritical airfoils (compare Section 7) or on airfoils with a larger relative thickness. In such cases flow separation occurs, starting at the airfoil trailing edge, and the maximum lift coefficient of the swept wing decreases compared to an unswept wing. This effect has already been expressed approximately in Section 7 by

$$C_{L,max,swept} = C_{L,max,unswept} \cdot \cos\varphi_{25} \quad .$$

The maximum lift coefficient with retracted flaps is estimated here according to **DATCOM 1978** (4.1.3.4 Method 2). This is an empirical method that may be applied in the subsonic range to untwisted tapered wings with a constant airfoil section over the span. The following must apply for the aspect ratio:

$$A > \frac{8}{3 \cdot \cos\varphi_{25}} \quad . \tag{8.2}$$

According to **DATCOM 1978** it is:

$$C_{L,max,clean} = \left(\frac{C_{L,max}}{c_{L,max}} \right) \cdot c_{L,max,clean} + \Delta C_{L,max} \quad . \tag{8.3}$$

This includes

$\left(\frac{C_{L,max}}{c_{L,max}} \right)$ stated in Fig. 8.9.

$c_{L,max}$ the maximum lift coefficient of the airfoil. $c_{L,max}$ is taken from measurements or airfoil catalogs. If, exceptionally, no measurements or airfoil catalog are available, equation (8.1) can be referred to.

$\Delta C_{L,max}$ Mach number correction term from Fig. 8.10. For Mach numbers smaller than 0.2

Δy *leading-edge sharpness parameter* as described above.

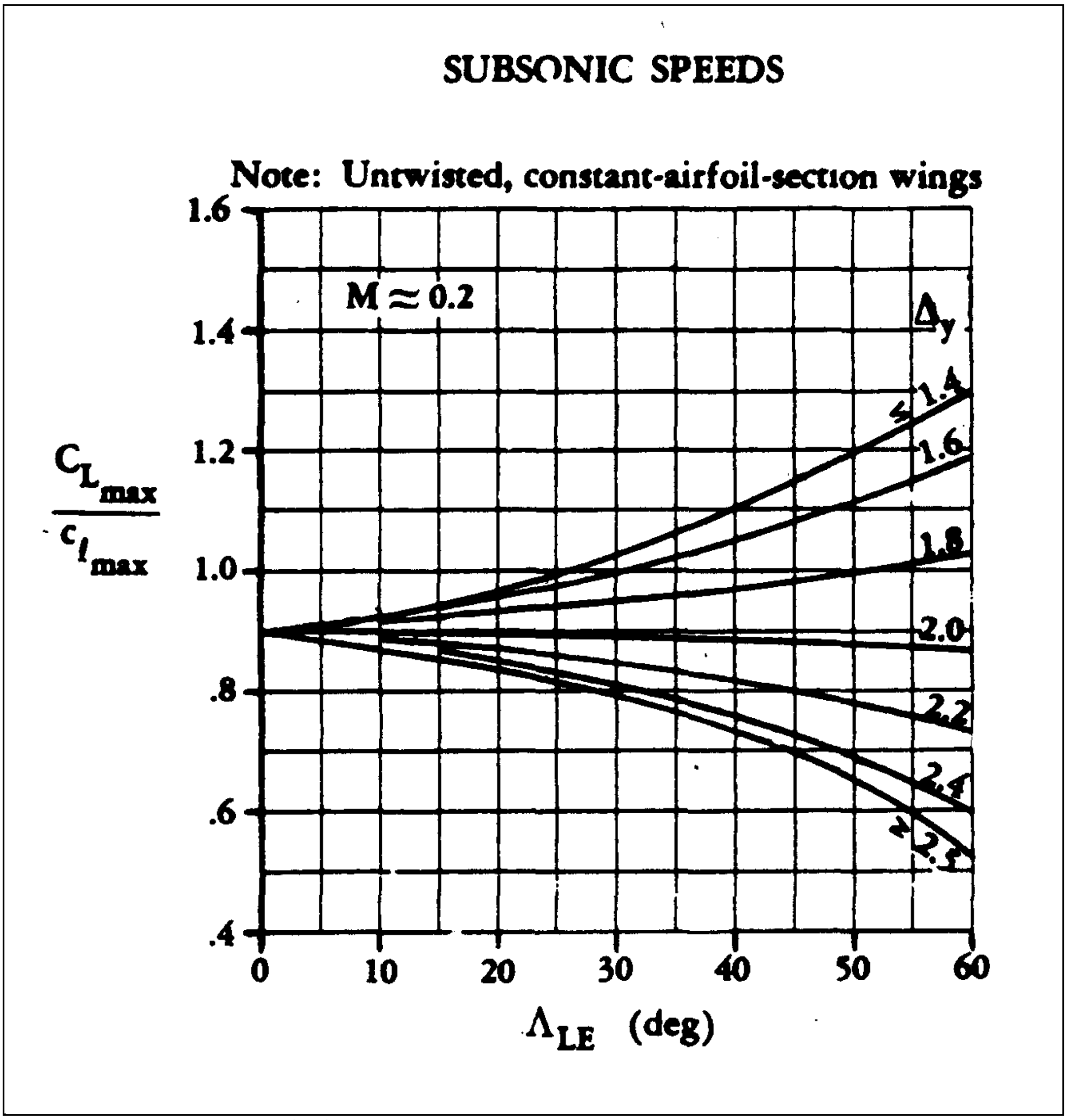

Fig. 8.9 Maximum lift of tapered wings with a high aspect ratio in subsonic speeds. Λ_{LE} stands for sweep angle of the leading edge φ_{LE} (**DATCOM 1978)**

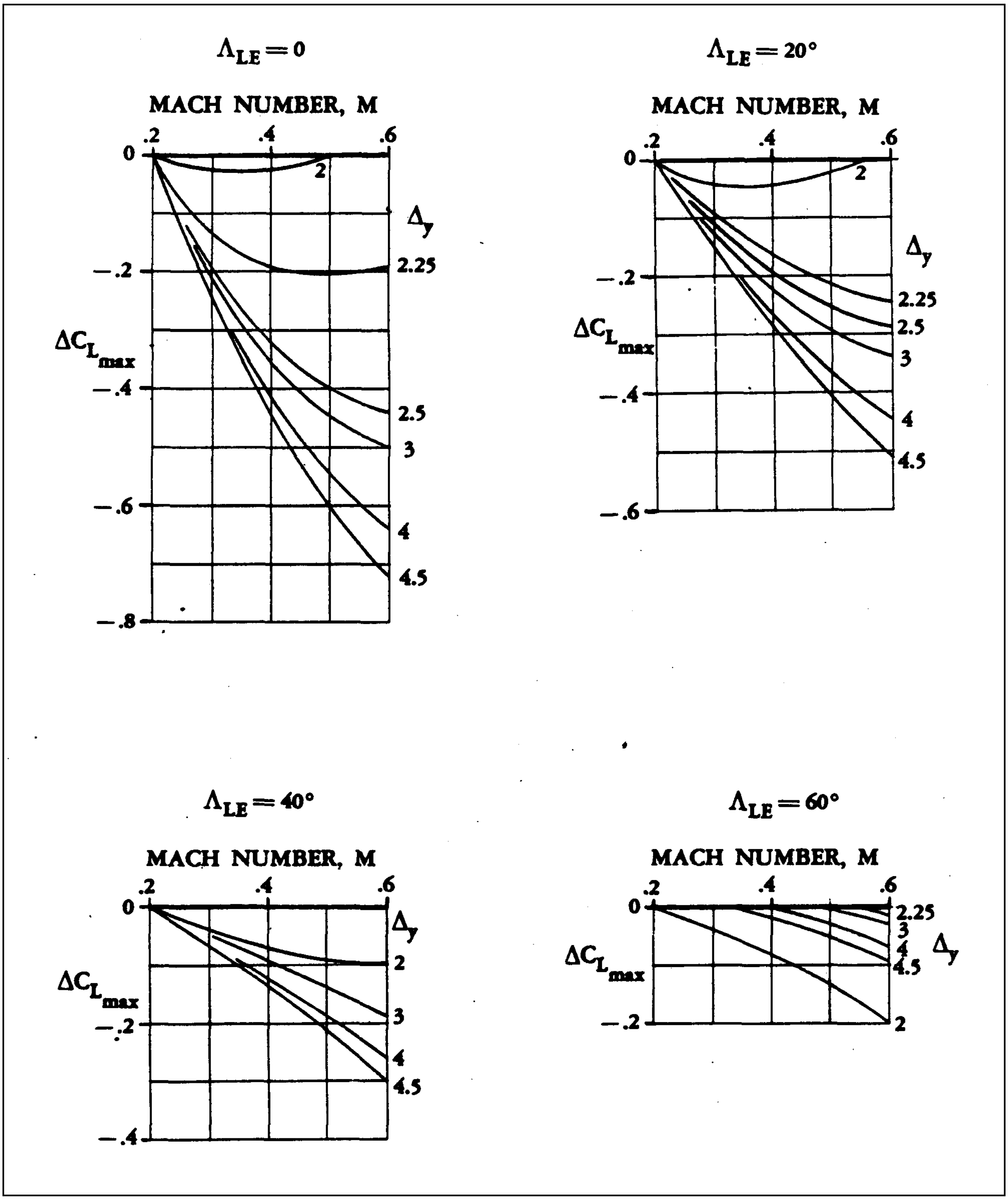

Fig. 8.10 Correction term $\Delta C_{L,max}$ to calculate the maximum lift of tapered wings with a high aspect ratio in subsonic speeds. Λ_{LE} stands for sweep angle of the leading edge φ_{LE} (**DATCOM 1978**). For Mach numbers smaller than 0.2 $\Delta C_{L,max}$ = 0.

Increase in maximum lift coefficient of an airfoil through high lift devices

The calculations are carried out according to **DATCOM 1978** (Section 6.1.1.3). The increase in the lift coefficient of the airfoil through **flaps on the airfoil trailing edge** is

$$\Delta c_{L,max,f} = k_1 \, k_2 \, k_3 \, (\Delta c_{L,max})_{base} \quad . \tag{8.4}$$

$(\Delta c_{L,max})_{base}$ is the maximum increase in the lift coefficient for a flap with a 25% flap chord according to Fig. 8.11 at a reference flap angle (according to Fig. 8.13).

k_1 is a factor according to Fig. 8.12, which takes into account a relative flap chord that has a value other than 25%.

k_2 is a factor according to Fig. 8.13, which takes into account a flap deflection that differs from the reference value according to Fig. 8.13.

k_3 is a factor according to Fig. 8.14, which takes into account the flap kinematics (Fig. 8.2).

The increase in the lift coefficient of the airfoil through **slats** or **flaps on the airfoil leading edge** can also be determined. The method *cannot* be applied to Kruger flaps; leading edge flaps can be calculated up to a deflection of 30° and slats up to a deflection of 20°. Above 20° an excessively high increase in the lift coefficient is calculated. It is

$$\Delta c_{L,max,s} = c_{l,\delta,max} \, \eta_{max} \, \eta_\delta \, \delta_f \, \frac{c'}{c} \, . \tag{8.5}$$

$c_{l,\delta,max}$ is the theoretically maximum flap efficiency according to Fig. 8.15.

η_{max} is an empirical factor according to Fig. 8.16 for taking into account the parameter "leading edge radius/relative thickness", $\frac{\mathrm{LER}}{t/c}$. The discontinuity in the curve for the slats is due to the fact that data from two different sources were used as the basis for the diagram.

η_δ is an empirical factor according to Fig. 8.17 for taking into account the actual angle of deflection compared to the optimum angle of deflection (reference angle).

δ_f is the angle of deflection of the slat or the leading edge flap pursuant to Fig. 8.18.

$\frac{c'}{c}$ is the ratio of the chord with and without deflection of the high lift aids on the airfoil leading edge pursuant to Fig. 8.18.

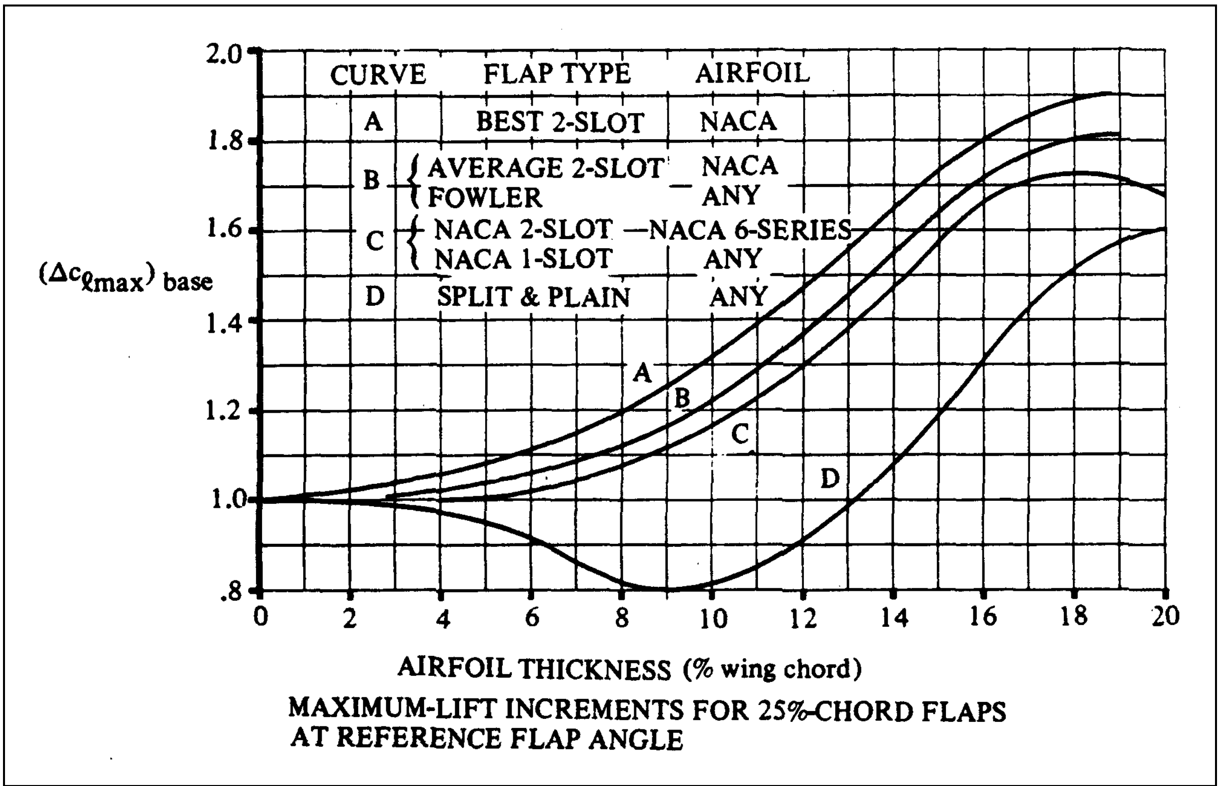

Fig. 8.11 Maximum increase in lift coefficient for 25%-chord flaps at a reference flap angle (according to Figure 8.13) (**DATCOM 1978**)

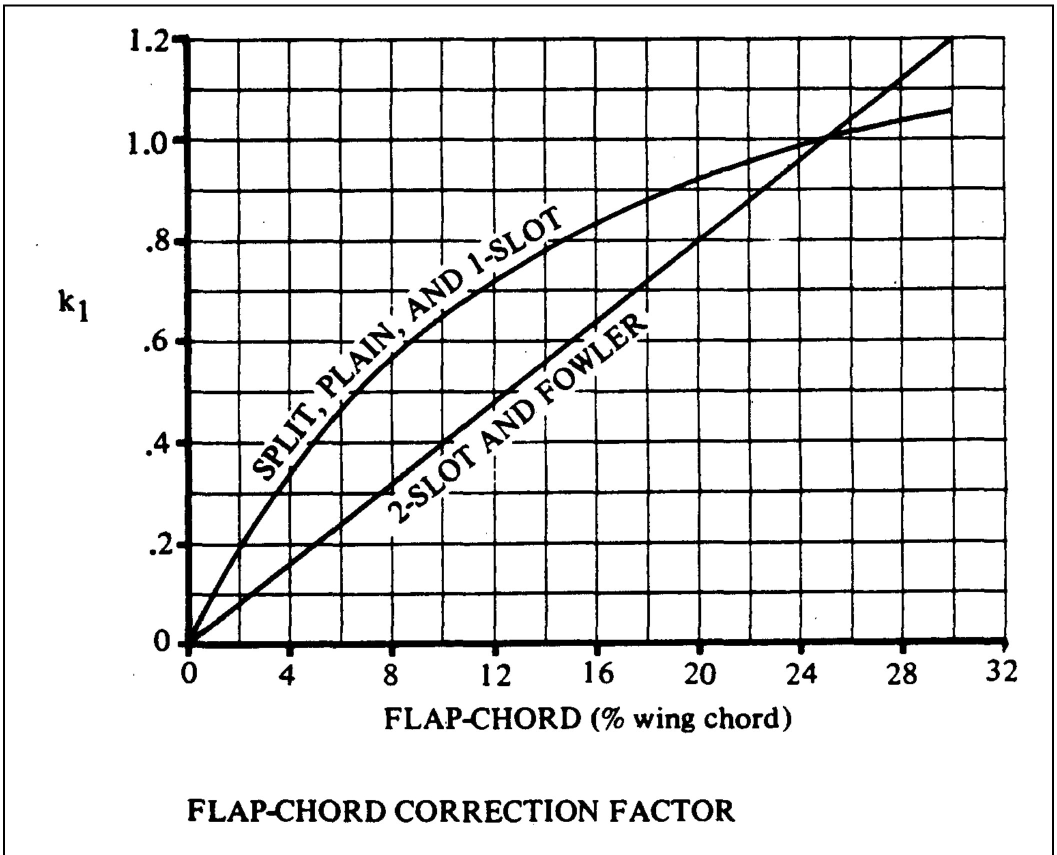

Fig. 8.12 Factor that takes the relative flap-chord into account, which has a different value then 25% (**DATCOM 1978**)

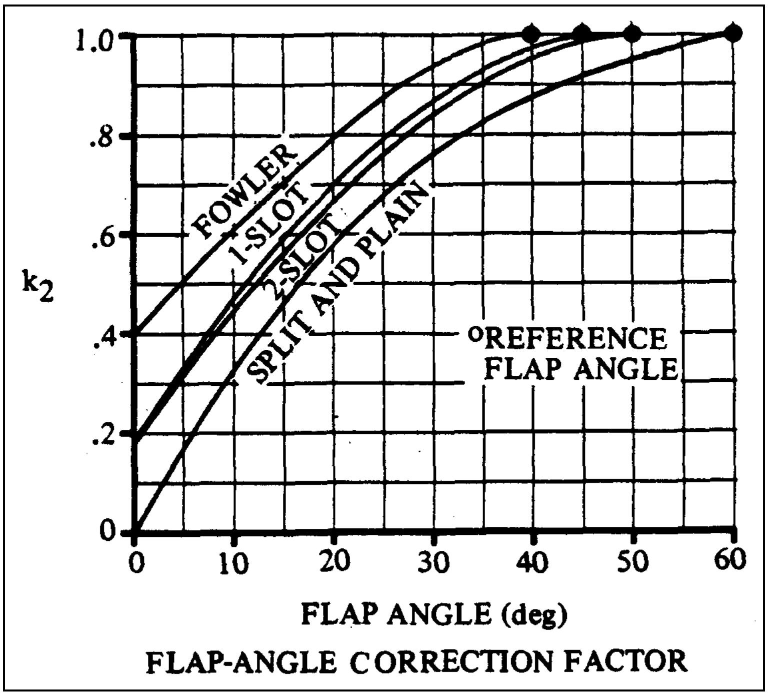

Fig. 8.13 Factor that takes the flap angle into account, which differ from the reference value (marked by • in the figure) (**DATCOM 1978**)

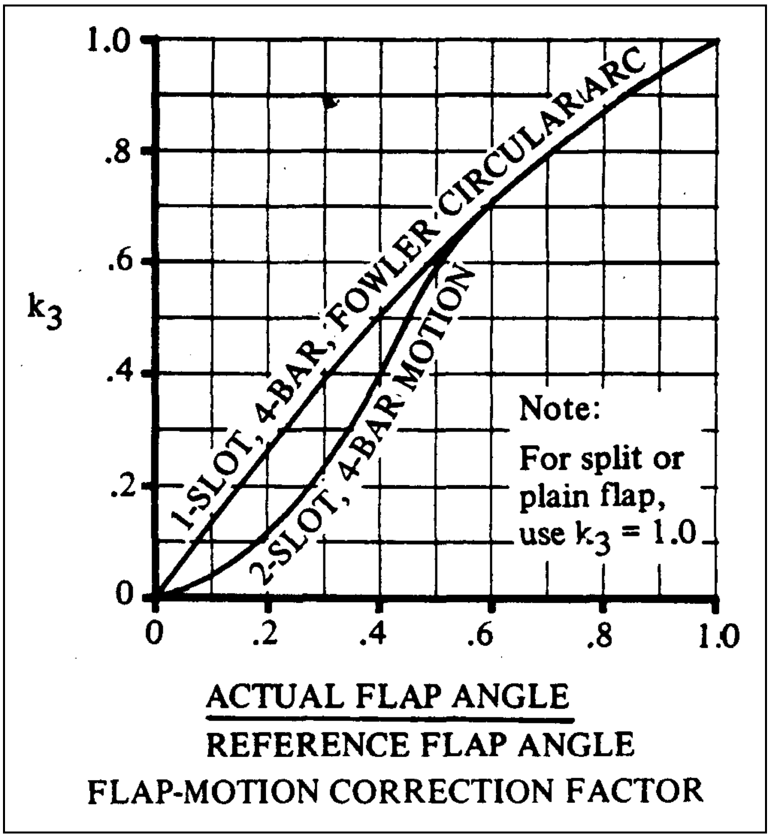

Fig. 8.14 Factor that takes the flap kinematics (see Fig. 8.2) into account (**DATCOM 1978**)

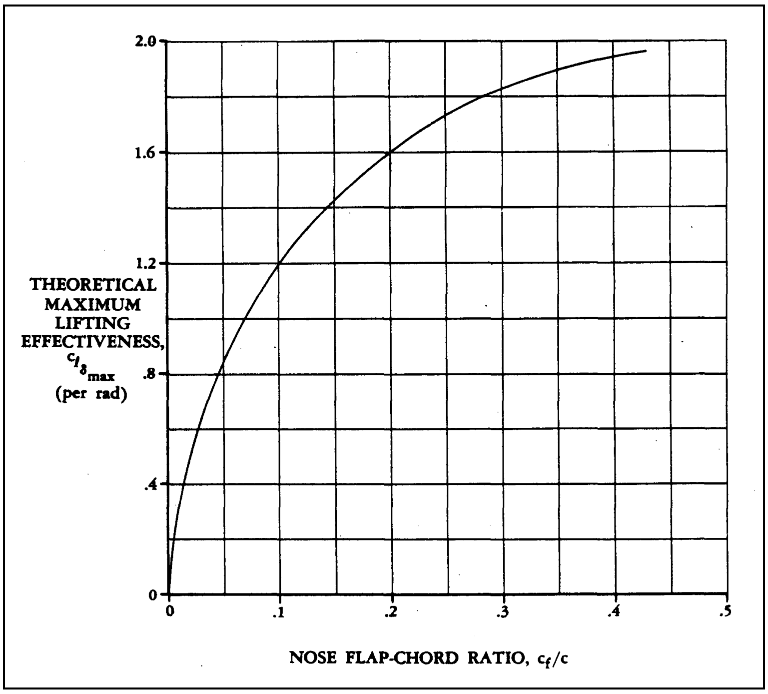

Fig. 8.15 Theoretical maximum flap effectiveness (**DATCOM 1978**)

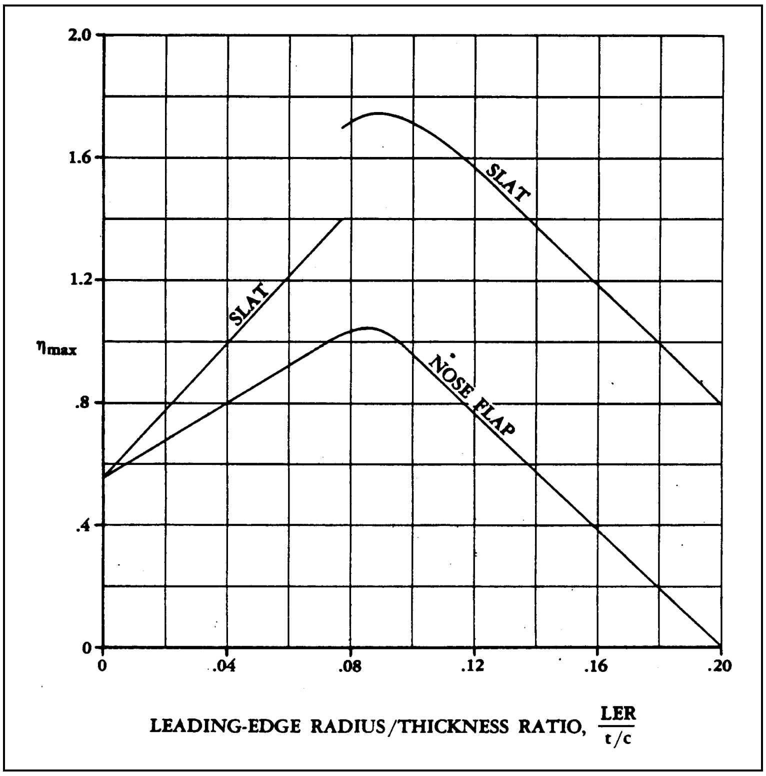

Fig. 8.16 Empirical factor that takes the value of "Leading-Edge Radius / Thickness Ratio", $\frac{\text{LER}}{t/c}$ into account. (**DATCOM 1978**)

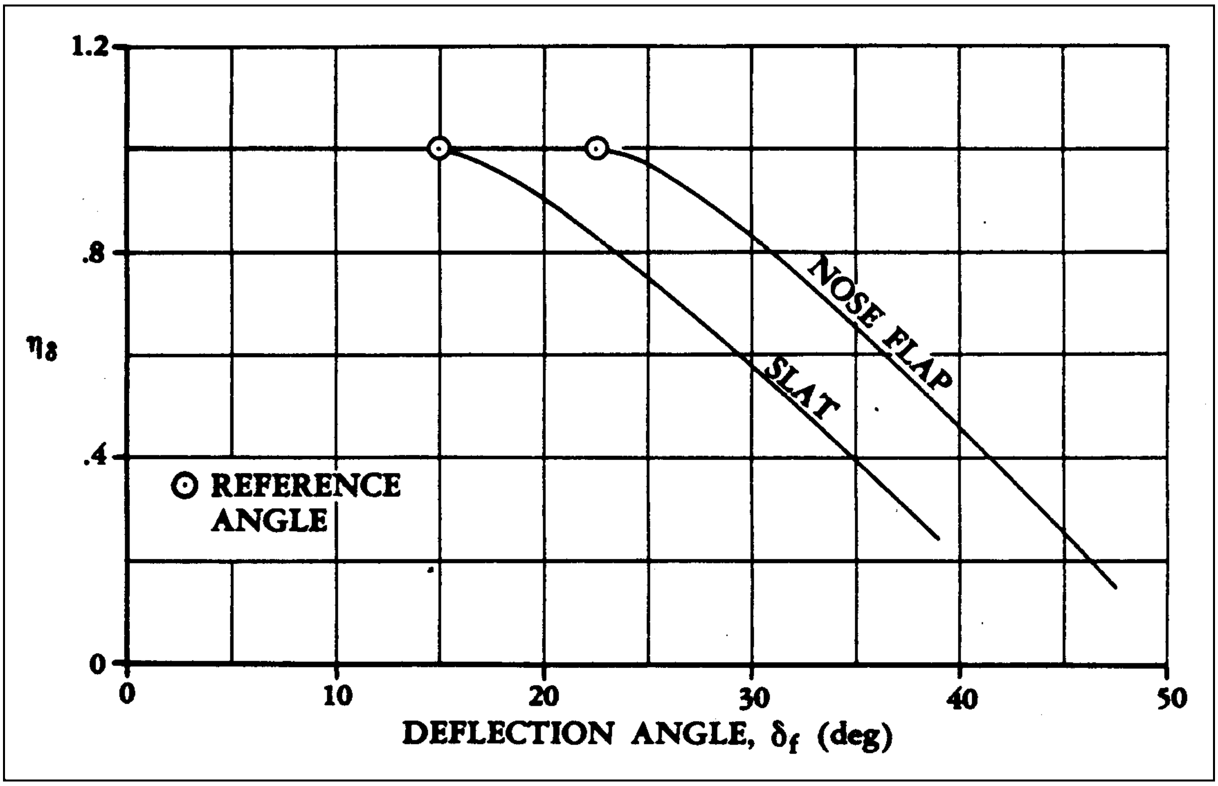

Fig. 8.17 Empirical factor that takes the real deflection angle in contrast to the optimum deflection angle (reference angle) into account (**DATCOM 1978**)

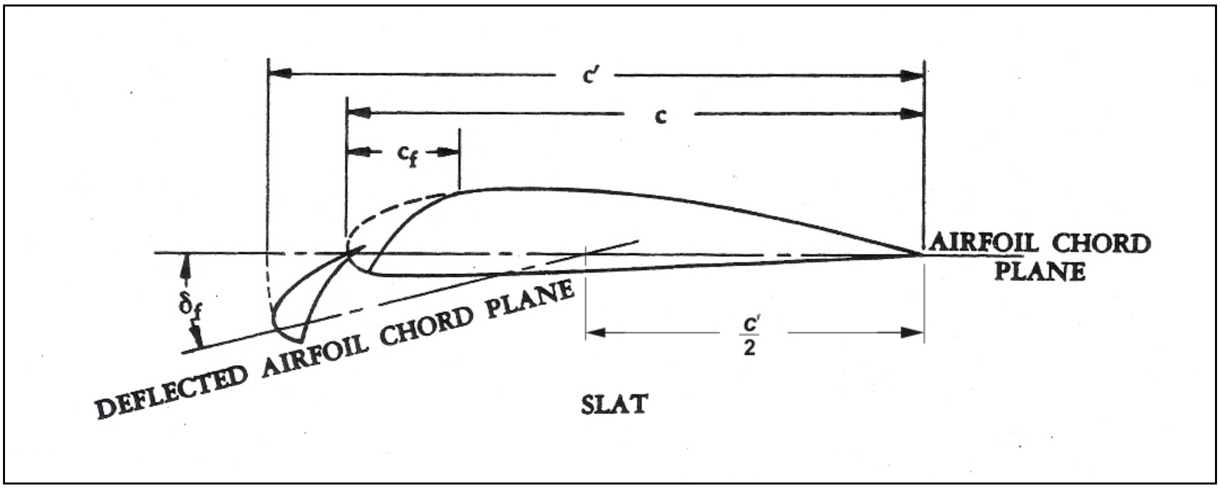

Fig. 8.18 Geometrical definitions of an airfoil with slat (adapted from **DATCOM 1978**). The airfoil chord line is defined with retracted slat. The slat is extended and rotated downwards. The slat deflection angle may be determined from the deflected airfoil chord line which is defined by the leading edge and the c'/2-point on the airfoil chord line.

Increase in the maximum lift coefficient of a wing through high lift devices

For flaps the calculation is carried out according to **DATCOM 1978** (6.1.4.3)

$$\Delta C_{L,max,f} = \Delta c_{L,max,f} \cdot \frac{S_{W,f}}{S_W} \cdot K_\Lambda \quad . \tag{8.6}$$

$\Delta c_{L,max,f}$ Increase in the maximum lift coefficient of the airfoil produced by flaps.

K_Λ an empirical correction factor according to Fig. 8.19 for taking into account the wing sweep φ_{25}.

$\frac{S_{W,f}}{S_W}$ Area ratio for the flaps according to Fig. 8.20.

For slats an estimate according to **Raymer 1992** is selected because **DATCOM 1978** does not contain a generally applicable method.

$$\Delta C_{L,max,s} = \Delta c_{L,max,s} \cdot \frac{S_{W,s}}{S_W} \cdot \cos\varphi_{H.L.} \quad . \tag{8.7}$$

$\Delta c_{L,max,s}$ Increase in the maximum lift coefficient of the airfoil produced by slats.

$\frac{S_{W,s}}{S_W}$ Area ratio for the slats. Calculation according to Fig. 8.20, only that in this case the hatching indicates the area that lies behind the slats.

$\varphi_{H.L.}$ Sweep angle of the **h**inge **l**ine of the slats.

The maximum lift coefficient of the wing is finally obtained from

$$C_{L,max} = C_{L,max,clean} + \Delta C_{L,max,f} + \Delta C_{L,max,s} \quad . \tag{8.8}$$

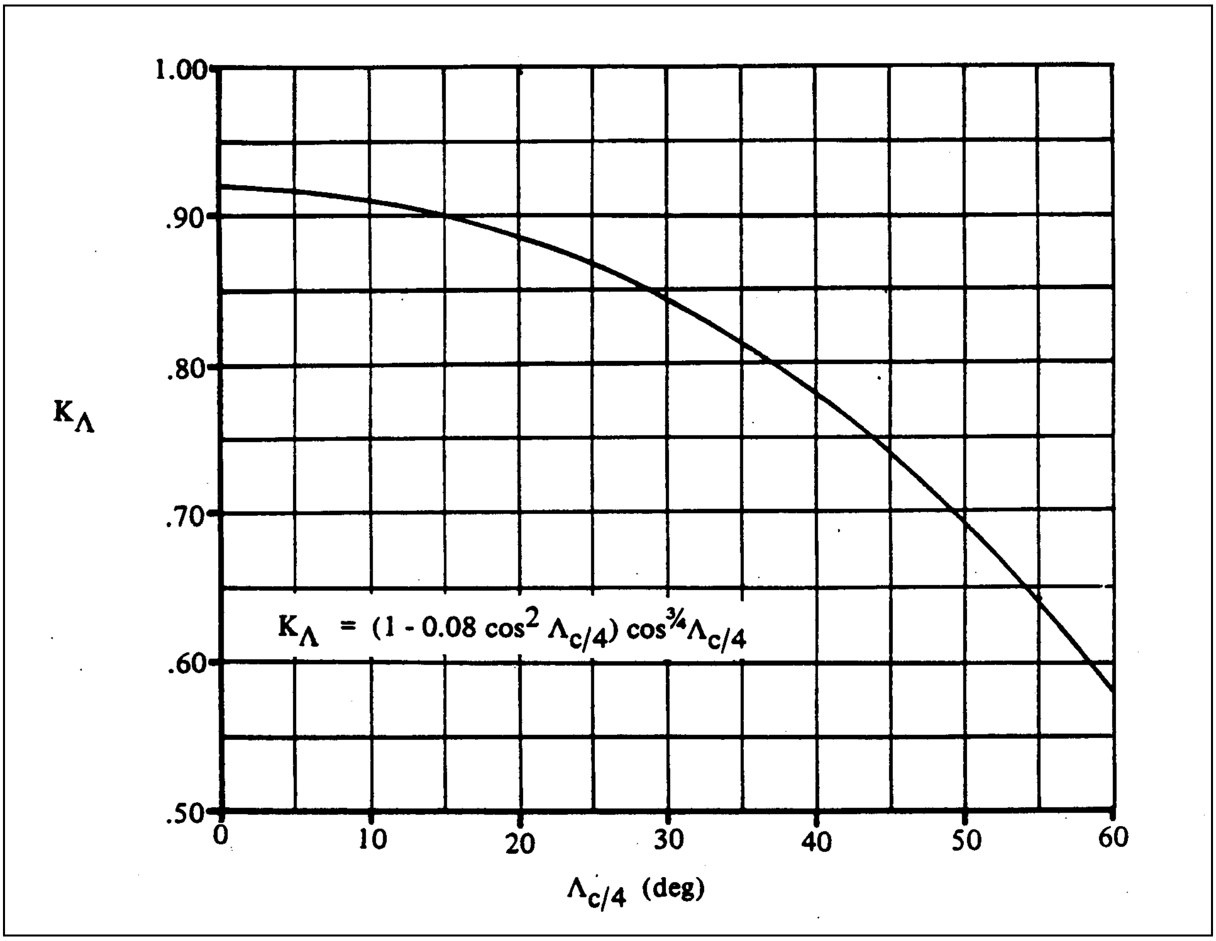

Fig. 8.19 Correction factor that takes the sweep into account $\Lambda_{c/4} = \varphi_{25}$ (**DATCOM 1978**)

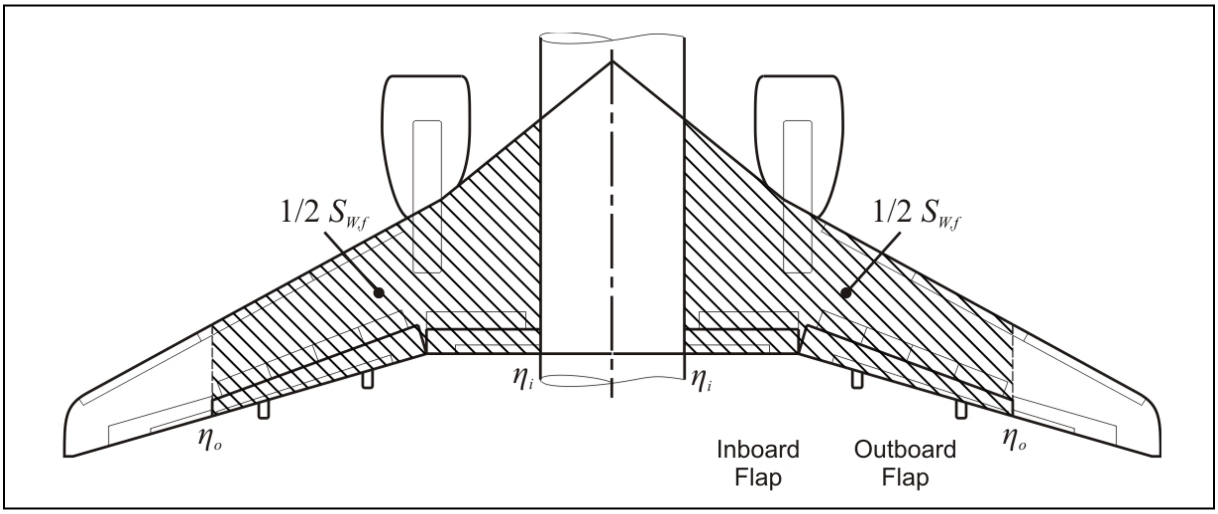

Fig. 8.20 Definition of $S_{W,f}$

8.3 Design of High Lift Systems

A simple conservative assumption can be adopted as maximum lift coefficient for the design of the wing, including the high lift systems:

$$C_{L,max} = 1.1 \cdot C_{L,max,INITIAL\ SIZING} \quad . \tag{8.9}$$

$C_{L,max,INITIAL\ SIZING}$ is the maximum lift coefficients assumed in Section 5 for preliminary sizing for take-off $C_{L,max,TO}$ and landing $C_{L,max,L}$

Factor **1.1** ensures that the aircraft can still stay in the air if the empennage creates negative lift to trim the aircraft.

The maximum lift coefficient for the wing $C_{L,max,clean}$ has already been established through the wing design in Section 7 – by means of the parameters found there – and can be calculated using the method from Subsection 8.2. On the basis of equation (8.8) the following is produced

$$0.95 \cdot \Delta C_{L,max,f} + \Delta C_{L,max,s} \geq C_{L,max} - C_{L,max,clean} \quad . \tag{8.10}$$

$C_{L,max}$ from equation (8.9).

Factor **0.95** takes into account the following interrelationship: the use of landing flaps creates a moment around the pitch axis. This moment must be compensated for by using trim. The negative lift created by the trim has to be balanced out by an additional lift of the wing.

As a result of factors 1.1 and 0.95 according to **Roskam II** in equation (8.9) and equation (8.10), the maximum wing lift is greater than $C_{L,max,INITIAL\ SIZING}$. This is necessary for a balanced sum of forces across the whole aircraft.

The aim of the design is now to determine the parameters of the high lift system in such a way that in equation (8.10) the left side is somewhat larger than (or at least the same as) the right side. To do this, the achievable lift must be distributed over the slats and flaps. The spanwise reach of slats and flaps has to be established, as must the flap type and the angle of deflection of slats and flaps. As already mentioned in Section 2, it will not generally be possible to set the parameters without an iterative approach.

The calculation methods used here largely stem from **DATCOM 1978**. DATCOM (data compendium) contains so-called *handbook methods* that produce a result relatively quickly. **DATCOM 1978** is a professional tool and has been repeatedly quoted by a large number of authors in the field of aircraft design for decades and is used for initial design steps. However, nowadays the detailed design of an aircraft requires considerably more precise information. This information can only be obtained by using detailed numerical methods and powerful computers.